Two-Dimensional Crystallization of a Histidine-Tagged Protein on Monolayers of Fluidity-Enhanced Ni^{2+}-Chelating Lipids

Sébastien Courty,[#,†] Luc Lebeau,[*,‡] Laurence Martel,[§] Pierre-François Lenné,[†] Fabrice Balavoine,[||] Wanda Dischert,[▽] Oleg Konovalov,[§] Charles Mioskowski,[||] Jean-François Legrand,[§] and Catherine Vénien-Bryan*[,⊥]

Institut de Biologie Structurale Jean-Pierre Ebel (CEA-CNRS), 41 rue J. Horowitz, 38027 Grenoble Cedex 1, France, Laboratoire de Chimie Organique Appliquée associé au CNRS, Université Louis Pasteur, 74 route du Rhin, 67401 Illkirch, France, UMR 5819 (CEA-CNRS-University J. Fourier), DRFMC/CEA-Grenoble, 17 av. des Martyrs, 38054 Grenoble Cedex 9, France, Laboratoire de Spectrométrie Physique, Université J. Fourier Grenoble 1-CNRS, BP 87, 38402 St Martin d'Hères, France, Service des Molécules Marquées, DBCM, CEA /Saclay, 91191 Gif sur Yvette, France, DBMS/CEA-Grenoble, 17 av. des Martyrs, 38054 Grenoble Cedex 9, France, and Laboratory of Molecular Biophysics, University of Oxford, South Parks Road, OX1 3QU Oxford, U.K.

Received July 18, 2002. In Final Form: September 19, 2002

Protein two-dimensional (2D) crystallization on lipid monolayers is a powerful method for structure determination. This method has been extended using the specific and strong interaction between histidine residues (of an overexpressed protein) and Ni^{2+} ions tethered at the headgroup of synthetic lipids. Understanding and then improving the process of adsorption and crystallization of proteins on a lipid monolayer are prerequisites for the production of large and well-ordered crystals of any soluble or membrane His-tagged proteins. These large high-quality arrays are necessary for structural studies at high resolution. We have investigated the steps of adsorption and 2D crystallization of His-HupR using three different lipids: (i) 2-(bis-carboxymethyl-amino)-6-[2-(1,3-di-*O*-oleyl-glyceroxy)-acetyl-amino] hexanoic acid nickel-(II) (Ni-NTA-DOGA), which has been previously used, and two specifically designed Ni^{2+}-chelating lipids, (ii) Ni-NTA-BB, which has two branched (B) alkyl chains and (iii) Ni-NTA-BF, a nonsymmetrical lipid with one branched (B) and one fluorinated (F) chain. These three lipids, when spread at the air−water interface, exhibit various fluidity properties. The adsorption and crystallization process have been monitored in situ and in real time using a variety of complementary techniques such as ellipsometry, shear rigidity measurements of the monolayer, and Brewster angle microscopy, and we have also developed X-ray reflectivity analysis to investigate the evolution of the electron density profile of the lipid−protein monolayer. Electron microscopy observations of the protein−lipid layers were also performed. We have found that the fluidity of the lipid monolayer has a marked influence on the rates of protein adsorption and crystallization of His-HupR. When Ni-NTA-BB is used to form the monolayer, it accelerates the process of protein adsorption and the protein crystallization is three times faster than when Ni-NTA-DOGA is used.

Introduction

The technique of two-dimensional (2D) crystallization of proteins on a lipid monolayer[1] has become a powerful technique in structural biology. About 30 soluble proteins have been crystallized by using surface-bound affinity ligands or surface-bound charged lipids (Coulombic interactions) (for reviews, see refs 2−4). A more recent extension of this technique exploits the interaction between a metal-coordinated lipid and a polyhistidine-tagged protein.[5−10] Structural analysis of the protein 2D crystals may be performed by electron crystallography. Near-atomic-resolution structures have been obtained from streptavidin crystals grown on biotinylated lipid monolayers.[11] Grazing incidence synchrotron X-ray diffraction[12−14] is an emerging method, which is also able to generate 3D models from protein 2D crystals. With the use of a high-resolution setup, it is possible to observe

* To whom correspondence should be addressed. E-mail addresses: lebeau@aspirine.u-strasbg.fr; venien@biop.ox.ac.uk.
[#] Institut de Biologie Structurale Jean-Pierre Ebel (CEA-CNRS).
[†] Université J. Fourier Grenoble 1-CNRS.
[‡] Université Louis Pasteur.
[§] UMR 5819 (CEA-CNRS-University J. Fourier).
[||] Service des Molécules Marquées, DBCM.
[▽] DBMS/CEA-Grenoble.
[⊥] University of Oxford.

(1) Uzgiris, E. E.; Kornberg, R. D. *Nature* **1983**, *301*, 125.
(2) Jap, B. K.; Zulauf, M.; Scheybani, T.; Hefti, A.; Baumeister, W.; Aebi, U.; Engel, A. *Ultramicroscopy* **1992**, *46*, 45.
(3) Lebeau, L.; Schultz, P.; Célia, H.; Mésini, P.; Nuss, S.; Klinger, C.; Olland, S.; Oudet, P.; Mioskowski, C. In *Handbook of nonmedical applications of liposomes*; Barenholz, Y., Lasic, D. D. E., Eds.; CRC Press: Boca Raton, FL, 1996; Vol. II, p 153.
(4) Ellis, M. J.; Hebert, H. *Micron* **2001**, *32*, 541.
(5) Kubalek, E. W.; Le Grice, S. F.; Brown, P. O. *J. Struct. Biol.* **1994**, *113*, 117.
(6) Barklis, E.; McDermott, J.; Wilkens, S.; Schabtach, E.; Schmid, M. F.; Fuller, S.; Karanjia, S.; Love, Z.; Jones, R.; Rui, Y.; Zhao, X.; Thompson, D. *EMBO J.* **1997**, *16*, 1199.
(7) Vénien-Bryan, C.; Balavoine, F.; Toussaint, B.; Mioskowski, C.; Hewat, E. A.; Helme, B.; Vignais, P. M. *J. Mol. Biol.* **1997**, *274*, 687.
(8) Vénien-Bryan, C.; Schertler, G. F. X.; Thouvenin, E.; Courty, C. *J. Mol. Biol.* **2000**, *296*, 863.
(9) Bischler, N.; Balavoine, F.; Milkereit, P.; Tschochner, H.; Mioskowski, C.; Schultz, P. *Biophys. J.* **1998**, *74*, 1522.
(10) Levy, D.; Chami, M.; Rigaud, J. L. *FEBS Lett.* **2001**, *504*, 187.
(11) Avila-Sakar, A. J.; Chiu, W. *Biophys. J.* **1996**, *70*, 57.
(12) Haas, H.; Brezesinski, G.; Mohwald, H. *Biophys. J.* **1995**, *68*, 312.
(13) Weygand, M.; Wetzer, B.; Pum, D.; Sleytr, U. B.; Cuvillier, N.; Kjaer, K.; Howes, P. B.; Losche, M. *Biophys. J.* **1999**, *76*, 458.
(14) Lenne, P. F.; Berge, B.; Renault, A.; Zakri, C.; Vénien-Bryan, C.; Courty, S.; Balavoine, F.; Bergsma-Schutter, W.; Brisson, A.; Grubel, G.; Boudet, N.; Konovalov, O.; Legrand, J. F. *Biophys. J.* **2000**, *79*, 496.

10.1021/la026261z CCC: $22.00
Published on Web 10/26/2002

narrow Bragg reflections, which indicate the possibility of structural determination at high resolution. This approach is complementary to electron crystallography with the advantage that the structure and the formation of protein complexes are investigated in situ.

The 2D crystallization technique is a versatile method. Among the multiplicity of applications is the possibility of crystallization of proteins over a wide range of molecular weights and also the possibility of cocrystallization of complexes. For instance, yeast RNA polymerase II with associated template DNA and product RNA has been crystallized and described.[15] It may also be possible to study large conformational changes because 2D crystals are accessible from the buffer solution, and in this particular geometry, more freedom is allowed for variation in molecular shapes than in 3D crystals. Another interesting development is the use of a lipid monolayer at the air−water interface, which can mimic the membrane surface. Some proteins might need to interact with the surface of the membrane to achieve their functional conformation. These contacts are important in a number of biological processes, such as immunoresponse, or signal transduction. The 2D crystallization technique on lipid monolayer is ideal for recreating the proper environment necessary for the active state of the protein. That strategy has been used for studying the structure and the function of a membrane-bound murine molecule expressed at the surface of cells the role of which is to present peptides to T cells.[16]

A very recent and exciting development of the technique enabled the 2D crystallization of a His-tagged membrane protein.[17] This new strategy is based on the use of partially fluorinated Ni^{2+}-chelating lipids that spread into stable monolayers at the air−water interface even in the presence of detergents. They were used to prepare 2D crystals of the plasma membrane H^+-ATPase from *Arabidopsis thaliana*.

Herein, we report on the design of some new amphiphiles with various hydrophobic chain characteristics that aim to modify the fluidity properties of the resulting monolayers. We have investigated the behavior of these new amphiphilic molecules at the air−water interface and their influence on the adsorption and crystallization steps of the His-HupR, a soluble transcriptional regulator from *Rhodobacter capsulatus*. The investigation was carried out using well-established techniques such as ellipsometry, shear rigidity measurements of the monolayer, and electron microscopy Brewster angle microscopy, but also we are presenting a new X-ray reflectivity study, which allowed us to analyze the electron density profile of the lipid−protein monolayer at the air−water interface during its formation.

Materials and Methods

Lipids and Proteins. Dioleoyl phosphatidylcholine (DOPC) was from Avanti Polar Lipids and Sigma. The 2-(bis-carboxymethyl-amino)-6-[2-(1,3-di-*O*-oleyl-glyceroxy)-acetyl-amino] hexanoic acid nickel(II) complex **1** (Ni-NTA-DOGA, Figure 1) was prepared as previously described.[7] Compounds **2** (Ni-NTA-BB, Figure 1) and **3** (Ni-NTA-BF, Figure 1) were prepared according to Figure 2. The secondary alcohols **4a** and **4b**[18] were reacted with

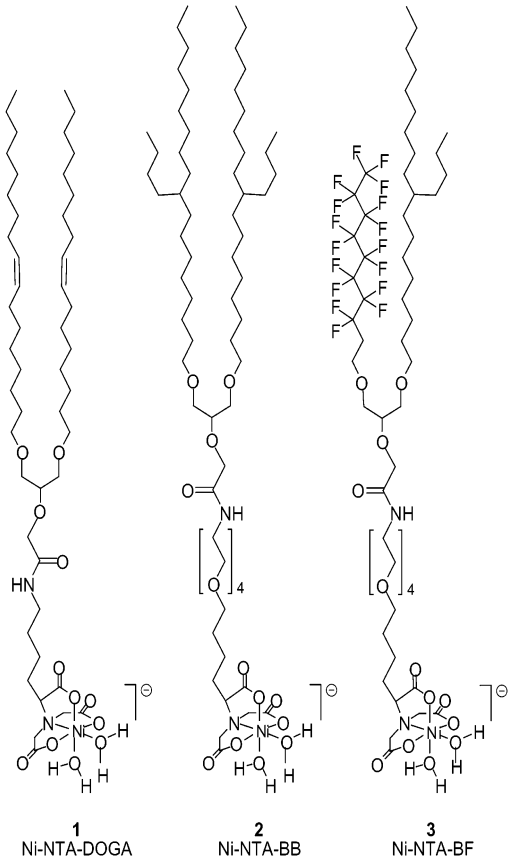

Figure 1. Structure of the three Ni^{2+} lipids used in this study: (**1**) Ni-NTA-DOGA; (**2**) Ni-NTA-BB, with two branched alkyl chains; (**3**) Ni-NTA-BF, with one branched and one fluorinated chain.

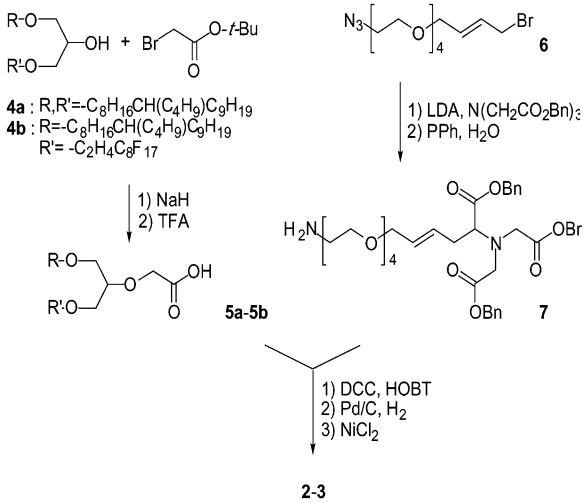

Figure 2. Synthetic scheme for the preparation of compounds **2** and **3**.

tert-butyl bromoacetate, and the resulting ethers were treated with trifluoroacetic acid to produce the corresponding carboxylic acids **5a** and **5b**. Bromide **6** was obtained by reacting 2-{2-[2-(2-azidoethoxy)ethoxy]ethoxy}-ethanol[19] with 1,4-dibromobutene. Alkylation of nitrilotriacetic acid tribenzyl ester with halide **6** and subsequent azide reduction led to the amino compound **7**, which was

(15) Poglitsch, C. L.; Meredith, G. D.; Gnatt, A. L.; Jensen, G. J.; Chang, W. H.; Fu, J.; Kornberg, R. D. *Cell* **1999**, *98*, 791.

(16) Celia, H.; Wilson-Kubalek, E.; Milligan, R. A.; Teyton, L. *Proc. Natl. Acad. Sci. U.S.A.* **1999**, *96*, 5634.

(17) Lebeau, L.; Lach, F.; Vénien-Bryan, C.; Renault, A.; Dietrich, J.; Jahn, T.; Palmgren, M. G.; Kuhlbrandt, W.; Mioskowski, C. *J. Mol. Biol.* **2001**, *308*, 639.

(18) Nuss, S.; Mioskowski, C.; Lebeau, L. *Chem. Phys. Lipids* **1999**, *103*, 21.

(19) Lebeau, L.; Oudet, P.; Mioskowski, C. *Helv. Chim. Acta* **1991**, *74*, 1697.

further acylated with **5a** and **5b** using a standard procedure. Hydrogenolysis of the resulting products followed by subsequent treatment with $NiCl_2$ afforded the target compounds **2** and **3**.

Stock solutions of the lipids were kept in chloroform at −18 °C under nitrogen. The working solutions were prepared in chloroform/ethanol 95:5 (v/v) at a final lipid concentration of 500 μM. The Ni^{2+} lipids were used pure or diluted with DOPC in various ratios (2:1, 1:1, 1:3, 1:6, and 1:12 mol/mol).

The HupR protein was expressed as a histidine-tagged protein in *Escherichia coli* strain BL21(DE3) from plasmid pRSA7 as described.[20] The pure His-HupR fraction was dialyzed in buffer A (0.25 M NaCl, 20 mM Tris-HCl, pH 8.0). The final protein concentration was 0.08−0.10 mg/mL. The His-HupR protein was aliquoted and stored at −80 °C and diluted when necessary in buffer A.

Ellipsometry and Surface Tension Measurements. The variation of the ellipsometric angle (δ) is a relevant probe for changes occurring at the air−water interface. It is essentially proportional to the amount of lipid and protein present at the interface. The ellipsometric measurements were carried out with a conventional ellipsometer using a He−Ne laser operating at 632.8 nm as described previously.[21] The sample trough (home-built 8 × 4 cm^2) was made of Teflon, and the volume of the subphase used was 8 mL. Basically, a lipid monolayer was spread at the air−water interface. Once equilibrium was reached, the protein was injected into the subphase. Homogenization of the solution was realized using a peristaltic pump. All of the experiments were carried out at room temperature. Surface tension was measured by the Wilhelmy method using a 1-cm-wide filter paper. For the determination of isothermal pressure versus molecular area curves, a Langmuir trough equipped with an electrobalance was used.

X-ray Reflectivity Measurements. The electron density profile of a lipid−protein monolayer at the air−water interface can be investigated with grazing incidence X-rays.[13,22] Indeed, the reflected intensity in the specular direction may be calculated as the Fourrier transform of the electron density gradient:

$$R(q) = R_F(q)|(1/\rho_\infty)\int_{-\infty}^{+\infty}[d\rho(z)/dz]\exp(-iqz)\,dz|^2$$

where $q = 4\pi \sin(\theta)/\lambda$ is the scattering vector, θ the incidence angle, λ is the wavelength, $\rho(z)$ is the electron density profile, ρ_∞ is the electron density of the buffer, and R_F is the Fresnel reflectivity from the sharp interface between two media.

X-ray reflectivity was measured using a rotating anode generator (Rigaku, 40 kV, 180 mA) with Cu Kα radiation (λ = 0.1541 nm) selected with a horizontally focusing Guinier monochromator (Ge(111)). The measurements were performed in the angular range from θ = 0.2° to θ = 2.0°, which provided a spatial resolution of 1.5 nm in the modeling of the electron density profile. Complementary test measurements were performed at the open undulator beamline ID10B of the European Synchrotron Radiation Facility (Grenoble, France) with a wavelength λ = 0.1384 nm, up to an angle θ = 3.0°, which provided a spatial resolution of 1.0 nm.[23]

Measurement of the Shear Elastic Constant. The 2D-rheometer setup uses the action of a light float (32 mg), which applies a rotational strain to the monolayer through a magnetic torque (with a pair of Helmholtz coils and a small magnetized pin placed in the middle of the float). This setup and the procedure for data analysis have been described previously.[21] The angular response was measured in amplitude and phase and was considered to reflect directly the rotational strain of the monolayer. The sensitivity in shear modulus determination was 0.16 mN/m. The experimental procedure was as follows: A lipid layer was spread at the air−water interface (this layer does not show any detectable resistance to the shear flow). The amplitude and phase of the mechanical response were then recorded at a fixed frequency, usually 5 Hz, as a function of time. After complete stabilization, the protein was injected into the subphase and the homogeneity completed using a peristaltic pump. After a few hours, a nonzero shear modulus was measured and the kinetics of the rigidification was followed up to stabilization. All of the experiments were performed at room temperature.

Brewster Angle Microscopy. The formation of the 2D crystals was monitored using a home-built Brewster angle microscope (BAM). The bare water interface produces no reflection of *p*-polarized light incident at Brewster's angle. When a covering layer even as thin as a molecular monolayer is introduced, *p*-polarized light is reflected and an image can be recorded.[24,25] In contrast to fluorescence microscopy, photolabeling of the protein is not necessary because the signal intensity of the BAM images increases with the layer thickness and the refractive index of the interfacial film. It has been demonstrated[26] that BAM allows the visualization of surface adsorption and aggregation of proteins and that a quantitative analysis of the image gray scale can provide a laterally resolved measurement of protein surface density. Briefly, the home-built Brewster angle microscope is mounted above the trough. The He−Ne laser light (Melles-Griot) of 10 mW was *p*-polarized with a polarizer at an incident angle of 53.12° with respect to the surface normal (Brewster angle value for the air−water interface). When a monomolecular film covers the surface, the reflected intensity increases and is collected by a lens system to form an image on a monochromatic CCD camera (Dage-MTI CCD camera, recording 768 × 581 pixels images on a videotape). The images of interest captured by a Scion frame grabber combined with a PC computer were then expanded to correct for the distortion due to the oblique view and filtered to reduce the diffraction fringes caused by the coherence of the laser light.

Electron Microscopy and Image Processing. At the end of the experiments, carbon-coated electron microscope grids were placed on top of the interface, withdrawn after a few minutes of adsorption, and negatively stained with 2% (w/v) uranyl acetate. Negatively stained specimens were examined in a Zeiss 10C electron microscope operating at 80 kV. Micrographs were recorded at a nominal magnification of 40 000×. Suitable areas were digitized using an Optronics drum scanner (P1000) at a sampling raster of 12.5 μm. Images were processed using the SEMPER 6 Plus software system.

(20) Toussaint, B.; de Sury d'Aspremont, R.; Delic-Attree, I.; Berchet, V.; Elsen, S.; Colbeau, A.; Dischert, W.; Lazzaroni, Y.; Vignais, P. M. *Mol. Microbiol.* **1997**, *26*, 927.

(21) Vénien-Bryan, C.; Lenne, P. F.; Zakri, C.; Renault, A.; Brisson, A.; Legrand, J. F.; Berge, B. *Biophys. J.* **1998**, *74*, 2649.

(22) Als-Nielsen, J.; Kjær, K. In *Phase transitions in soft condensed matter*; Riste, T., Sherrington, D. e., Eds.; Plenum Press: New York, 1989; p 113.

(23) Konovalov, O.; Myagkov, I.; Struth, B.; Lohner, K. *Eur. Biophys J.*, in press.

(24) Hénon, S.; Meunier, J. *Rev. Sci. Instrum.* **1991**, *62*, 936.

(25) Hönig, D.; Möbius, D. *J. Phys. Chem.* **1991**, *95*, 4590.

(26) Frey, W.; Schief, W. R., Jr.; Vogel, V. *Langmuir* **1996**, *12*, 1312.

Results

Lipid Monolayers. A major goal in the present work was to investigate the relationship between the fluidity properties of the lipid matrix used as a template in protein 2D crystallization experiments and the crystallization kinetics and quality of the 2D crystals produced.

There are different ways to modulate the fluidity of a lipid monolayer. The cohesive interactions between the fatty chains of the lipid molecules associated with the hydrophobic effect can be partly altered through (a) a modification of electrostatic interactions between the polar heads of the lipids or between these polar heads and the bulk solvent[27−30] or (b) a change in the structure of the hydrophobic chains of the lipids.

To improve the production and possibly the quality of the His-tagged HupR crystals, we have designed and synthesized two original Ni^{2+}-chelating lipids (Figure 1, compounds **2** and **3**). Most of the lipids used in protein 2D crystallization incorporate two oleyl or oleoyl chains in their hydrocarbon skeleton.[2,3] Unsaturated chains adopt a bent conformation that partly prevents their tight packing inside the monolayer and thus provide the matrix with valuable fluidity properties. The reference compound Ni-NTA-DOGA (Figure 1, compound **1**) is one of these lipids and has been previously used for the 2D crystallization of His-HupR.[7] Ni-NTA-BB **2** and Ni-NTA-BF **3** were designed in such a way that they spread into stable but more fluid monolayers at the air−water interface. Various approaches were used and combined to prevent the tight packing of the lipid chains in the monolayer: (a) breaking the linear geometry of the chains (branched chain B), (b) breaking the symmetry of the molecule (two different chains on the same scaffold), and (c) introducing aliphatic chains with both hydrophobic and lipophobic properties (fluorinated chain F). In the latter case, a regular packing of the chains inside the monolayer is avoided and, because of the nonideality of hydrocarbon−fluorocarbon mixtures,[31,32] the overall monolayer cohesion is reduced as statistically each chain can only establish cohesive interactions with half of the neighboring chains. Then the monolayer cohesion results from B−B and F−F interactions, whereas B−F interactions are repulsive, hence improving the monolayer fluidity. Moreover, compounds **2** and **3** have been designed with the addition of a tetra(ethylene glycol) spacer (between the hydrophobic moiety and the Ni^{2+} ligand) the flexibility of which is expected to facilitate protein reorientation when anchored to the lipid monolayer.

The hydrophobic scaffold of Ni-NTA-BB has been previously used elsewhere to investigate the 2D crystallization of the B subunit of DNA gyrase.[32] For that particular purpose, it was anchored to an antibiotic (novobiocin) and the resulting conjugated lipid was shown to accelerate the process of 2D crystallization compared with a lipid incorporating two unsaturated chains. However, no systematic in situ measurements have been conducted during that study, and the derivatized lipid was only used for the study of DNA gyrase.

Lipid Monolayer Isotherms. Surface pressure versus molecular area isotherms are sensitive to changes in molecular organization of amphiphiles at the air−water interface. Isotherms obtained with the compounds investigated in that study were measured at 20 °C using buffer A (Figure 3A). No main phase transition plateau is observed for any of the lipids indicating that they all collapse in the fluid phase at room temperature, which is a prerequisite for further protein 2D crystallization. The fluidity of the lipid layers is ensured at 20 °C by the unsaturation (compound **1**) and the branch (compounds **2** and **3**) in the aliphatic chain, which prevent tight liquid crystalline packing. Just before the collapse, the areas per lipid molecule are 46 $Å^2$ for compound **1** (the reference lipid Ni-NTA-DOGA) and 55 and 72 $Å^2$ for compounds **2** (Ni-NTA-BB) and **3** (Ni-NTA-BF), respectively. These values, though not determined with a high accuracy, do highlight that branching and fluorination of the hydrophobic tails do prevent the tight packing of the lipid molecules.

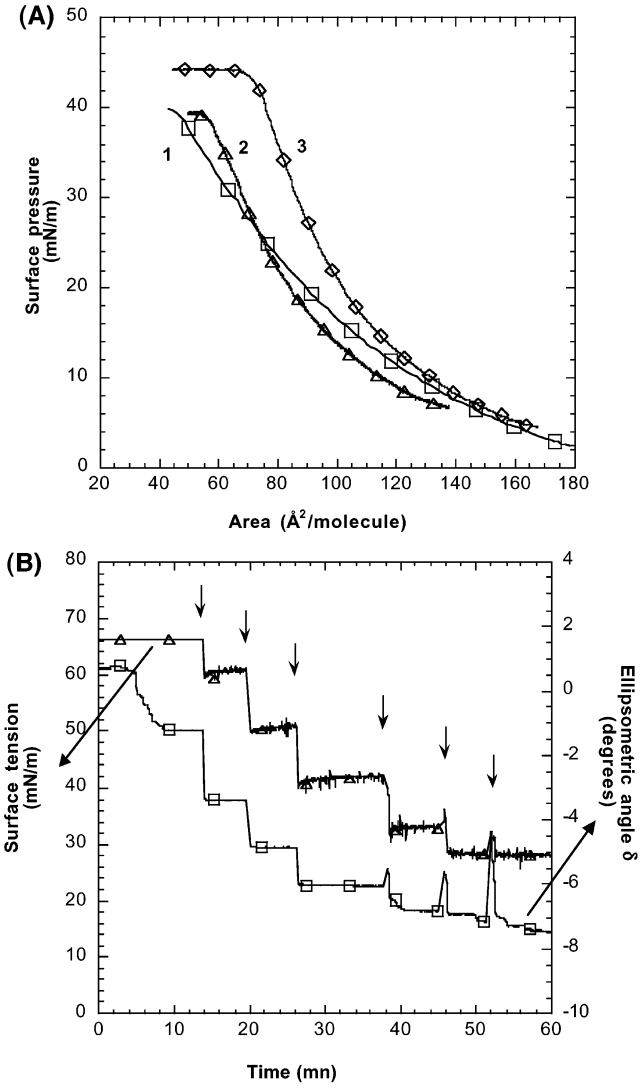

Figure 3. Isothermal surface pressure versus lipid molecular area (A) for compounds **1** Ni-NTA-DOGA (□), **2** NI−NTA-BB (△), and **3** Ni-NTA-BF (◇) at 21 °C and (B) Surface tension (△) and ellipsometric angle (□) versus time for Ni-NTA-BF. Each arrow represents an injection of lipids.

Ellipsometric Studies. The variations of the ellipsometric angle and of the surface tension during sequential delivery of a Ni-NTA-BF solution at the interface were recorded (Figure 3B). These measurements allow the determination of the exact amount of lipid required to obtain a fully dense monolayer at the maximum surface pressure that the monolayer can sustain. Such a fully

(27) Lebeau, L.; Mioskowski, C.; Oudet, P. *Biochim. Biophys. Acta* **1988**, *939*, 417.
(28) Scherer, P. G.; Seelig, J. *Biochemistry* **1989**, *28*, 7720.
(29) Hauser, H. *Chem. Phys. Lipids* **1991**, *57*, 309.
(30) Lohner, K. *Chem. Phys. Lipids* **1991**, *57*, 341.
(31) Murkerjee, P. *Colloids Surf.* **1994**, *A84*, 1.
(32) Lebeau, L.; Nuss, S.; Schultz, P.; Oudet, P.; Mioskowski, C. *Chem. Phys. Lipids* **1999**, *103*, 37.

dense state is definitely necessary to allow further successful 2D crystallization experiments. Loose monolayers have been revealed to be unstable during the protein attachment process.[3] We then always worked with a slight excess of lipids compared to the previous value (ca. 10%). The necessity of this excess of lipid is due to the existence of the "border effects" where there is a partial accumulation of lipid molecules at the edges of the trough (this phenomenon is particularly acute when small troughs are used). These "extra" lipids form some reservoirs that can compensate for some lipid depletion from the monolayer resulting from protein−lipid interaction.[3] The amount of lipid needed to reach the minimum surface tension and the maximum variation of the ellipsometric angle is the same. The final stabilized value remains constant for at least 48 h (data not shown). Ni-NTA-DOGA **1** and Ni-NTA-BB **2** show a similar behavior (data not shown). The overall variation of $\delta = -7° \pm 2°$ was obtained in the ellipsometry experiments for the three different lipids, and the surface pressure measurements show very similar values as well: 40 mN/m for Ni-NTA-DOGA **1** and Ni-NTA-BB **2** (data not shown) and 38 mN/m for Ni-NTA-BF **3** (Figure 3B). It has to be stressed that the sign of the variation of δ is arbitrary, and in that particular case, it is deliberately chosen to be negative to facilitate the reading of Figure 3B. All three monolayers also show remarkable stability over extended periods of time.

Adsorption and Crystallization of His-HupR on a Ni-NTA-DOGA/DOPC Lipid Monolayer. The ellipsometric angle, δ, and the shear elastic constant, μ, were recorded as functions of time for the lipid mixture Ni-NTA-DOGA/DOPC 1:3 (mol/mol), the protein concentration in the subphase being 25 μg/mL (Figure 4A). The ellipsometric angle is proportional to the quantity of protein adsorbed to the lipid monolayer. The lipid monolayer contribution to δ is $7° \pm 2°$ (vide supra) and has been subtracted in Figure 4A. After protein injection, we observed first a lag between 20 and 30 min followed by a period during which the ellipsometric angle $\Delta\delta$ fluctuates but increases and reaches a value of 20° after about 3 h (see also Figure 7C). The fluctuation period corresponds to the formation of patches of well-packed proteins drifting under the laser footprint (the diameter of the laser beam is about 2 mm). It is possible to image these well-packed proteins using BAM: some bright areas are drifting on the surface until they percolate (see Figure 8 and Courty thesis[33]). After 3 h, the adsorption of a monolayer of HupR appears to be completed. An evaluation of the surface density can be obtained from comparison with streptavidin monolayers, which give an ellipsometric angle value of 16° for a surface density of 3.2 mg m^{-2}.[14] Using the same ratio of 0.2 mg m^{-2} deg^{-1}, we obtain 22° for the plateau value of the ellipsometric angle with a surface density of 4.4 mg m^{-2}, which is close to that of a HupR 2D crystal: 4.9 mg m^{-2} with an area of 1810 Å^2 per protein.[8]

To further analyze the crystallization process of the protein monolayer, we have used a mechanical device that allows us to monitor the appearance of rigidity in situ and in real time (see Materials and Methods). The lipid mixture used is still Ni-NTA-DOGA/DOPC 1:3. The shear elastic modulus, μ, has a nonzero value after a delay of 3.5 h. This rigidity is expected to appear when crystallites have grown sufficiently to touch each other. Then, a mechanical percolation of 2D crystals over the whole area between the float and the edges of the trough takes place. After 14 h, the shear elastic constant reaches 40 mN/m and still increases, but at a slower rate, for about 10 h to reach the value of 58 mN/m. This should correspond to coalescence of the small crystallites and to an overall increase of the degree of crystallinity in the monolayer. Such a description is in agreement with in situ grazing incidence synchrotron X-ray diffraction results,[14] which have shown that HupR monolayers with high 2D crystalline order at the surface of water also exhibit a high shear modulus. Hence, after transfer onto electron microscope grids at the end of the experiments, large 2D crystals are observed (Figure 4B).

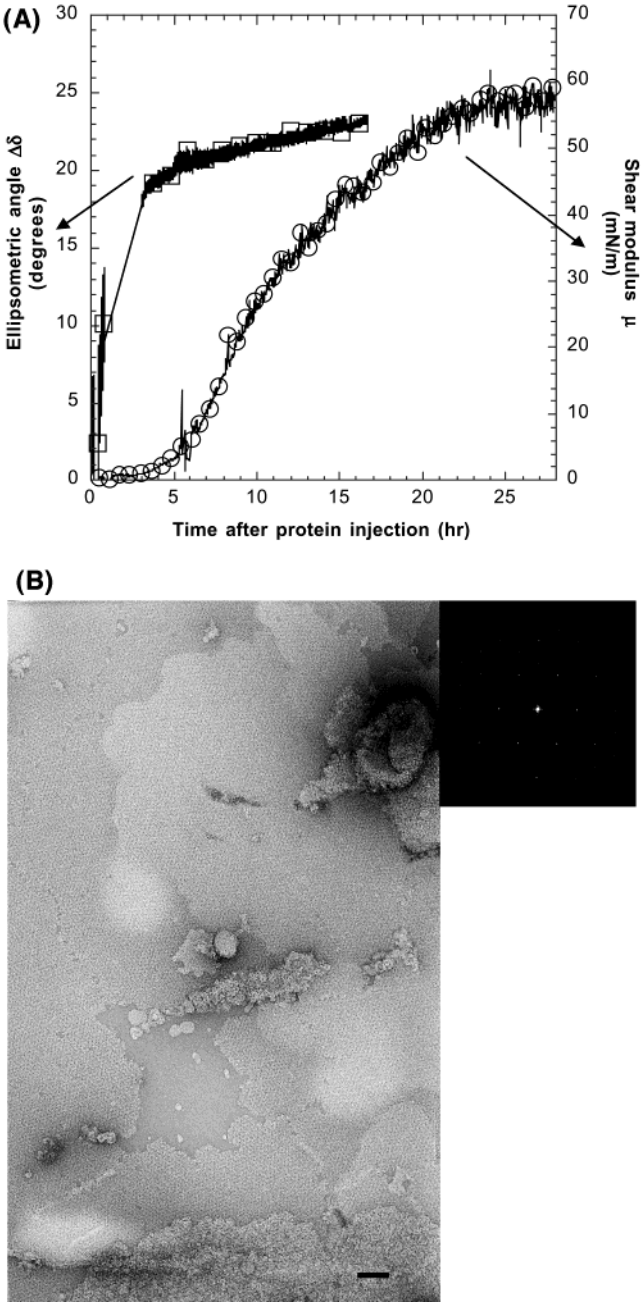

Figure 4. A standard case with His-HupR (25 μg/mL) and Ni-NTA-DOGA/DOPC 1:3 (mol/mol): (A) Ellipsometric angle $\Delta\delta$ (□) and shear elastic constant μ (○) versus time; (B) electron micrograph showing large crystalline areas of negatively stained crystals observed after transfer onto an electron microscope grid at the end of the experiment. The inset shows the diffraction pattern of the HupR crystals. The bar represents 100 nm.

Influence of the Ratio Ni-NTA-DOGA/DOPC on the Adsorption and Crystallization of His-HupR. The lipid ligand Ni-NTA-DOGA was mixed with DOPC in

(33) Courty, S. Solides bi-dimensionnels à l'interface air-eau: measures mécaniques et optiques. Ph.D. Thesis., University of Grenoble I, France, 2001.

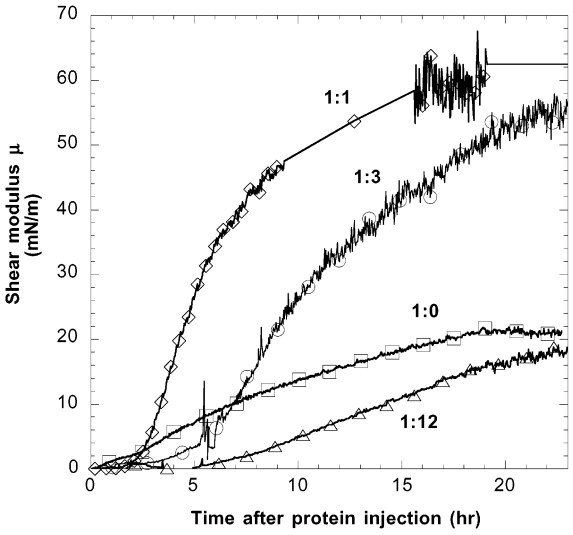

Figure 5. Influence of the lipid dilution ratio on the shear elastic constant. The lipid film (Ni-NTA-DOGA/DOPC (mol/mol) (□) 1:0; (◇) 1:1; (○) 1:3; (△) 1:12) is incubated with His-HupR at 25 μg/mL.

chloroform/ethanol 95:5 (v/v). Working solutions (500 μM) were prepared at various Ni-NTA-DOGA/DOPC final ratios (2:1, 1:0, 1:1, 1:3, 1:6, and 1:12 mol/mol). The protein concentration in the subphase was kept constant (25 μg/mL).

For monolayers made with Ni-NTA-DOGA/DOPC 1:1, 1:3, and 1:6 mol/mol, the shear modulus, μ, measured at the end of the incubation period with the protein was 58 $\pm$ 3 mN/m (Figure 5 and Table 1). After transfer of the layers (formed with the ratio 1:1, 1:3, and 1:6) onto electron microscope grids, some large and well-organized crystals were observed. The shear elastic constant starts to increase after 2 and 3.5 h for Ni-NTA-DOGA/DOPC 1:1 and Ni-NTA-DOGA/DOPC 1:3, respectively. The 1:1 ratio allows more protein to adsorb faster onto the lipid layer, so the whole crystallization process is accelerated. It is noteworthy that a monolayer spread from pure Ni-NTA-DOGA (1:0) leads to a low value of the shear modulus (20 mN/m, measured after 24 h). The Ni-NTA-DOGA/DOPC 1:12 mixture gives a shear modulus value even lower (18 mN/m). Although a high density of protein is obtained on the grids from the pure Ni-NTA-DOGA experiment, only very small crystals, if any, can be found. In the case of the 1:12 ratio, the surface density of the adsorbed protein appears to be too low to allow the proper protein−protein contacts necessary for 2D crystals to grow. This is indeed confirmed by electron microscopy because fewer proteins are seen on the specimen grids after transfer and no crystals are present (data not shown). On the basis of the dimension of HupR in the 2D crystal structure, the area of one molecule is about 1810 Å^2,[8] while the area per lipid ligand is ca. 50 Å^2. Therefore, in principle, a dilution ratio (Ni-NTA-DOGA/DOPC) 1:35 would provide enough ligands for binding a whole protein monolayer. Actually it appears that such a low concentration of ligand at the interface is not favorable to the formation of stable protein−lipid monolayers and therefore is not conducive to protein crystallization. Indeed, isolated protein−lipid complexes can be easily drawn from the interface to the aqueous subphase if lateral protein−protein interactions cannot be established fast enough so that it stabilizes the system.

Influence of pH, Imidazole, and Ni^{2+}-Lipid-Free Monolayer on the Crystallization Process. To give a final evidence that a specific Ni^{2+}−His-tag interaction is involved in the adsorption process of His-HupR to the Ni-NTA-DOGA monolayer, we have monitored in situ and in real time the adsorption and desorption of HupR to and from the lipid monolayer under various conditions. We have found that no adsorption of His-HupR was observed when the lipid monolayer was spread from pure DOPC (Figure 6A) or when imidazole (200 mM) was present in the trough prior to incubation with the protein (Figure 6B). In the latter case, the Ni^{2+} complex is chelated with imidazole and is no longer available for binding with the protein His-tag (in the protein purification protocol, 200 mM imidazole is used to make a competitive elution of the His-HupR from the Hitrap chelating column). We have observed both the effects of a pH variation and the addition of imidazole on preformed 2D crystals as well. Injection of concentrated HCl into the subphase to lower pH to 6.5 once the crystals are formed on the lipid monolayer led to rapid protein desorption from the lipid film (Figure 6A, arrow c). The proper interaction between histidine and a Ni^{2+} complex occurs in the pH range 7.5−8.5. Because the pK_a of histidine is close to 7.0, at pH 6.5 nearly 50% of these amino acid residues are protonated. Thus the interaction with the Ni^{2+} complex is canceled, and the protein can easily detach from the lipid monolayer. Interestingly, the injection of imidazole (200 mM final, arrow b, Figure 6B) after the crystals have been formed did not provoke any major desorption of His-HupR crystals. However, the observation of the specimens after transfer showed that the crystals were smaller and contained multiple defects (data not shown). A partial complexation of the Ni^{2+} ion with imidazole occurs because the interaction with imidazole is weaker than that with hexahistidine ($K_d = 10^{-8}$ M compared with 10^{-13} M at pH 8[34]). In addition, the cohesive force within a crystal resulting from protein−protein interactions contributes to prevent a massive desorption of the protein. However, the preformed crystals are weakened and do not transfer well on the electron microscope grids where they indeed appear small and patchy.

Monolayers Formed with Ni-NTA-BB and Ni-NTA-BF: Influence on the Adsorption and Crystallization of His-HupR. We have observed the mechanical properties of the monolayers of pure Ni-NTA-BB and Ni-NTA-BF (Figure 7A). The data corresponding to pure Ni-NTA-DOGA are shown as well for comparison. The protein concentration in the subphase is 25 μg/mL. The variation in time of lateral crystalline order is comparable between Ni-NTA-DOGA and Ni-NTA-BB, the maximum value for the shear elastic constant being 20 and 18 mN/m, respectively. The time at which half this value is obtained is 5 h. The variation of the shear elastic constant with time is different when pure Ni-NTA-BF is used. The delay until a nonzero value is obtained is about the same when compared with the other lipids, but a final value of 48 mN/m for the shear elastic constant μ is found, and the $t_{1/2}$ value is 4 h. In all of these three conditions, observations on the electron microscope grids after transfer of the monolayer are the same: the protein surface density is high, but very few and very small crystals are present, if any.

Figure 7B enables us to compare the crystallization behavior of His-HupR when the three different Ni^{2+} lipids are used, and in each case, they are diluted with DOPC at a ratio leading to crystallization (1:1). The striking feature is the constant final value of the shear elasticity (58 $\pm$ 3 mN/m) obtained whichever Ni^{2+} lipid is used. This particular value is suggesting the full coverage of the lipid

(34) Schmitt, J.; Hess, H.; Stunnenberg, H. G. *Mol. Biol. Rep.* **1993**, *18*, 223.

Table 1. Kinetics Details of the 2D Crystallization Process of the His-HupR Protein on Different Lipid Monolayers

lipid monolayer composition (mol/mol)	delay before adsorption ±0.2 h	delay before the in-plane rigidity increase ±0.3 h	maximum shear modulus value (mN/m) ±3 mN/m	$t_{1/2}$ for shear modulus ±0.3 h	presence of crystals on the EM grids
		Ni-NTA-DOGA/DOPC			
1:0	0	0.5	20	5	no
2:1					no
1:1		2.0	61	5.5	yes
1:3	0.3	3.5	58	10.5	yes
1:6			58		yes
1:12		6	18	14	no
		Ni-NTA-BB/DOPC			
1:0	0	0.5	18	5	no
2:1					no
1:1	0	0.1	56	3	yes
1:3	0	0.1	56	3	yes
1:12		3	18	9	no
		Ni-NTA-BF/DOPC			
1:0	0	0.5	48	4	no
2:1					no
1:1	0	3	58	7.5	yes
1:3	0.2	4	43	12	no
1:6		9	16	17	no
1:12			2		no

film with protein crystals, as confirmed by electron microscopy (Figure 4B). However, the kinetics of the crystallization depend on the Ni^{2+} lipid used. The $t_{1/2}$ values were 3, 5.5, and 7.5 h for Ni-NTA-BB/DOPC 1:1, Ni-NTA-DOGA/DOPC 1:1, and Ni-NTA-BF/DOPC 1:1, respectively. The Ni-NTA-BB/DOPC 1:1 mixture accelerates the crystallization process by a factor of about 2 when compared with Ni-NTA-DOGA/DOPC 1:1. The acceleration of the crystallization kinetics is even more important with the 1:3 lipid ratio (see Table 1).

Figure 7C enables us to compare the kinetics of adsorption of His-HupR when two different lipids diluted with DOPC at a 1:3 ratio (conducive to crystallization) are used. The maximum ellipsometric angle values obtained for both lipids, Ni-NTA-DOGA and Ni-NTA-BB, are comparable (23° ± 3° after 4 h), showing that lipid−protein layers have similar thickness. Nevertheless, the kinetics of adsorption are different. The in situ measurements allowed us to measure two things: (a) the delay, if any, before the adsorption of the protein and (b) the kinetics of adsorption of the protein. The delay before the ellipsometric angle value increases ranges from 20 to 30 min for Ni-NTA-DOGA/DOPC 1:3 and is nonexistent for Ni-NTA-BB/DOPC (1:0, 1:1, or 1:3).

Observation of the Surface Monolayer by Brewster Angle Microscopy. It is possible to monitor the formation of crystals of HupR with the Brewster angle microscope (BAM). The main contrast arises from the formation of a thin layer with a refractive index different from that of the subphase. Moreover, inside the lipid−protein monolayer, the 2D crystals are denser and thus give an additional contrast with respect to the noncrystalline surrounding domains. A set of pictures recorded with the video camera over time is shown in Figure 8A−D ($t = 0$ is when the protein is injected in the subphase). The lipid monolayer composition is Ni-NTA-DOGA/DOPC 1:3. The formation of crystals is clearly seen as bright spots on the dark background. The crystals grow in size, and the number of crystals increases with time. These bright patches are drifting on the surface until they percolate. The lipid ratios Ni-NTA-BB/DOPC 1:1 and Ni-NTA-BF/DOPC 1:3 and 1:1 do not have any influence on the size and number of crystals seen with the BAM, but they have some on the crystallization kinetics. The rate is 3 times faster when using Ni-NTA-BB/DOPC 1:3 when compared with NTA-DOGA/DOPC 1:3. There is an excellent correlation between the BAM observations and the presence of HupR crystals as observed on the electron microscope grids after transfer. No signal was observed when Ni-NTA-BF/DOPC 1:3 was used as confirmed by the absence of crystals on the electron microscope grids after transfer when that lipid mixture is used.

X-ray Reflectivity Analysis of the Monolayer Formation. We obtained X-ray reflectivity data during the adsorption and crystallization of His-HupR on Ni lipid monolayer as follows. After spreading Ni-NTA-DOGA/DOPC 1:3 on the surface of the His-HupR protein solution (25 μg/m in buffer A), we measured the reflected X-ray intensities over a limited range of angles. These data are shown in Figure 9A. Note that the protein solution was homogenized before the spreading of the lipids unlike the ellipsometry and shear modulus experiments in which the protein was injected and homogenized after the spreading of the lipid monolayer. Each set of measurements took place over 135 min and was made within the angular range where the first order of the Kiessig fringes[35] arising from a protein monolayer was expected. The first set of reflected intensity measurements (at the beginning of the incubation) is similar to the measurements made from a pure air/liquid interface. Indeed, within this angular range, the (X-ray beam) reflected intensity is not sensitive to the presence of the thin lipid monolayer. After 2 h, the intensity increases until it reaches a maximum after 14 h. The time evolution (of the surface coverage) at different fixed angles is presented in Figure 9B. The observed homothetic behavior can be modeled by a layer of fixed thickness $d \approx 85$ Å, of which the average electron density δ evolves linearly with the surface coverage c of the protein:

$$\delta = \delta_f c + \delta_s(1 - c)$$

where δ_s is the density of the buffer solution and δ_f is the final density of the protein monolayer. All of the data of Figure 9B can thus be analyzed with a single-exponential behavior:

$$c = 1 - \exp(-t/\tau)$$

with time constant $\tau = 4 \pm 0.5$ h, which corresponds to a value of $t_{1/2} = \tau \ln 2 = 2.8 \pm 0.3$ h.

(35) Kiessig, H. *Ann. Phys. Leipzig* **1931**, *10*, 769.

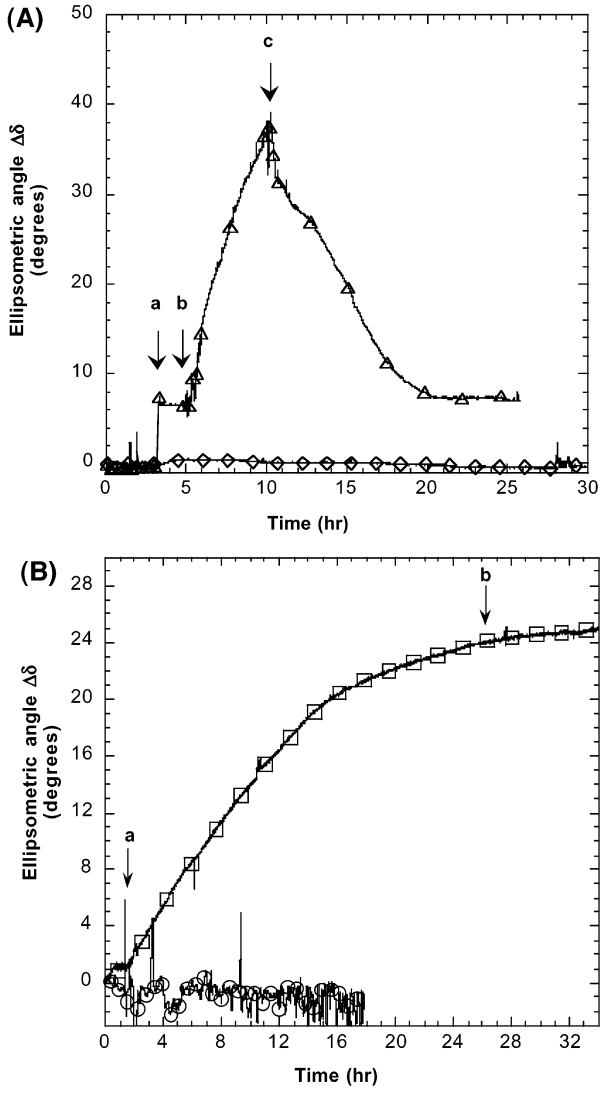

Figure 6. Film adsorption and desorption of the HupR protein under different conditions: (A) incubation of the protein (15 μg/mL) with (◇) a pure DOPC monolayer and (△) a Ni-NTA-DOGA/DOPC 1:3 monolayer. The crystallization takes place as follows: (arrow a) lipid spreading at the interface; (arrow b) HupR injection into the subphase; after 10 h, the pH value is lowered to 6.5 (arrow c, injection of HCl into the subphase). Panel B shows (○) a Ni-NTA-DOGA/DOPC 1:3 monolayer incubated with HupR (15 μg/mL) and imidazole and (□) incubation of the protein (15 μg/mL) with a Ni-NTA-DOGA/DOPC 1:3 monolayer. Spreading of the lipid corresponds to $t = 0$. The protein is injected into the subphase after 1 h (arrow a). Imidazole (200 mM final concentration, arrow b) is added into the subphase after a 25 h incubation period.

This characteristic time for adsorption $t_{1/2}$ is relatively long when compared to the results of Figure 4A in which the same mixture of lipids has been used (Ni-NTA-DOGA/DOPC 1:3) and $t_{1/2}$ is 1 h. This is attributed to the absence of circulation of the protein solution for homogenization during the reflectivity measurements.

Measurements of the reflectivity curve were also performed over a wider angular range (Figure 10). Each point of this curve was obtained by scanning the angle of detector around the specular direction and subsequent fitting of the reflected intensity with Gaussian function to subtract the background level. The analysis of the whole reflectivity curve was performed with a three-layer model: one for the hydrophobic tails of the lipid monolayer, the second for the hydrophilic heads of the lipids, and the last layer for the proteins (see inset Figure 10). A matrix

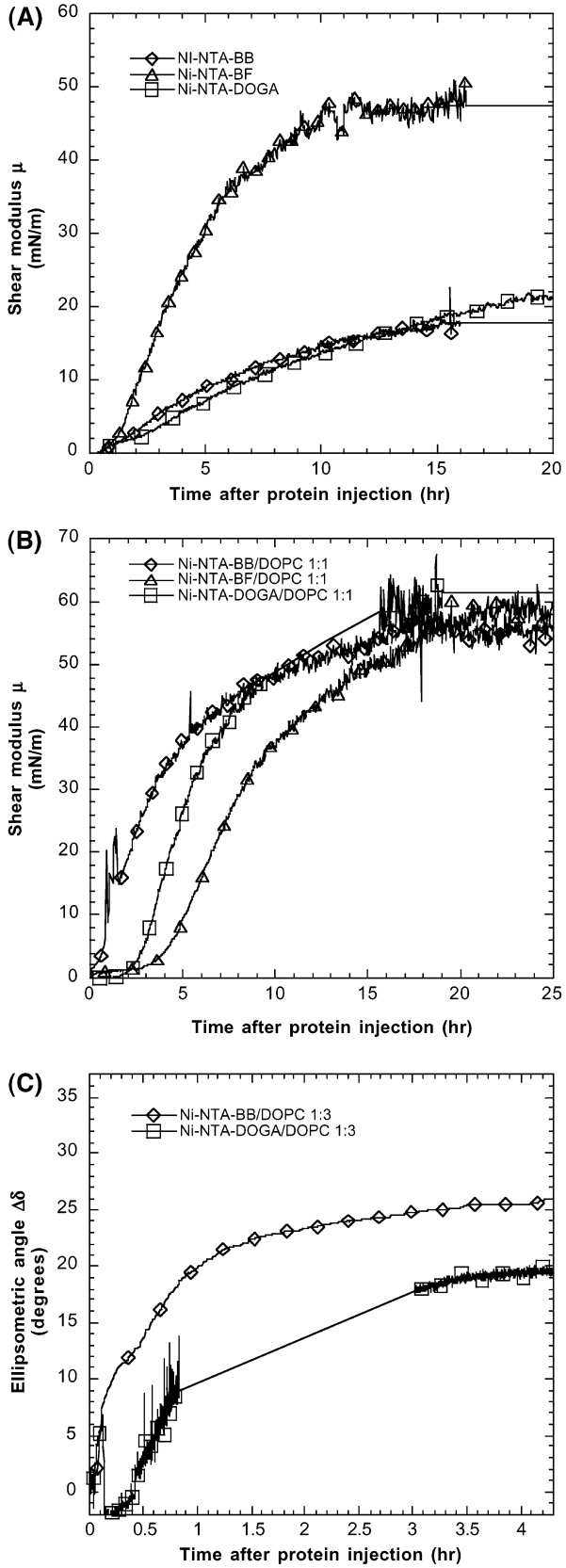

Figure 7. Influence of the lipid structure on the His-HupR crystallization process. The protein concentration is 25 μg/mL. Panel A shows the shear elastic constant μ versus time. The monolayer is made with pure lipid: (□) Ni-NTA-DOGA; (◇) Ni-NTA-BB; (△) Ni-NTA-BF. Panel B shows the shear elastic constant μ versus time for (□) Ni-NTA-DOGA/DOPC 1:1, (◇) Ni-NTA-BB/DOPC 1:1, and (△) Ni-NTA-BF/DOPC 1:1. Panel C shows the ellipsometric angle $\Delta\delta$ versus time for (□) Ni-NTA-DOGA/DOPC 1:3 and (◇) Ni-NTA-BB/DOPC 1:3.

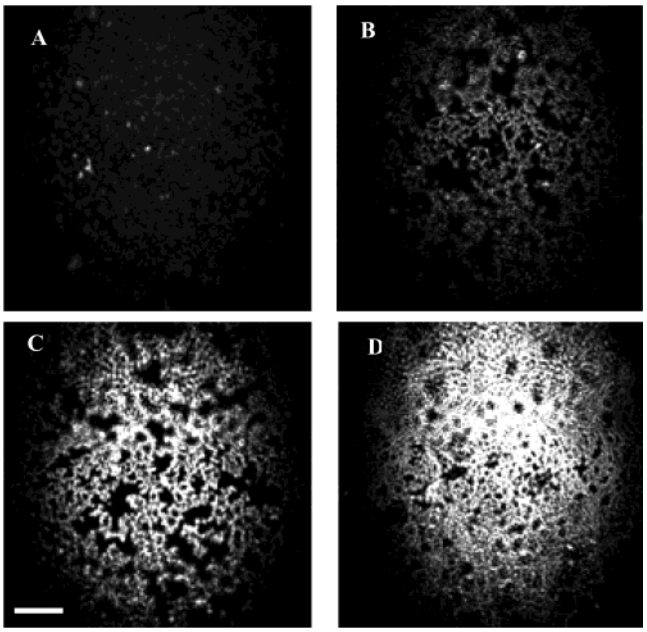

Figure 8. Brewster angle images taken during His-HupR crystallization on a Ni-NTA-DOGA/DOC 1:3 lipid monolayer. The concentration of the protein is 25 μg/mL. Incubation times were (A) 1, (B) 3, (C) 9, and (D) 18 h. The bar represents 100 μm.

formalism developed by Parratt[36] was used for the reflectivity calculations. The variable parameters of the model were the thickness and the electron density of each layer. The roughness of the various interfaces was assumed equal and was also adjusted. The results are shown Figure 10, and the parameters of the fit are given Table 2.

Monolayers formed with Ni-NTA-BB and Ni-NTA-BF have also been investigated using the X-ray reflectivity technique at ESRF. Figure 11 displays reflectivity curves of a lipid layer Ni-NTA-BB/DOPC 1:3 before and after incubation with the HupR protein solution during 12 h (25 μg/mL, buffer A). The results are analyzed as follows: The fit of the first curve obtained with the lipid layer alone gives the electron density profile of the lipid layer, and these parameters are used in the fit of the second curve to determine the thickness and the average electron density of the protein layer. The results are shown in Figure 11, and the parameters of the fit are given Table 2. A similar procedure was used with the lipid layer made of Ni-NTA-BF/DOPC 1:1 before and after incubation with the HupR protein. The results show a much weaker contrast between the different layers, probably due to the higher electron density of the partly fluorinated hydrophobic tails of the lipids (data not shown).

Comparison of the results obtained for the three lipid−protein layers, first, confirm that in the three situations contributing to 2D crystallization a single layer of HupR protein of 85 Å of thickness is bound to the lipid ligand monolayer. Second, it provides an estimation of the thickness and electron density of the lipid layers. Especially, the results of Table 2 show that the branched lipid layer Ni-NTA-BB/DOPC 1:3 has a 10% lower density than the layer of Ni-NTA-DOGA/DOPC 1:3, thus suggesting a higher fluidity of the former. Note in Table 2 that the thickness of the lipid head is larger in the mixture Ni-NTA-BB/DOPC 1:3 than in the mixture Ni-NTA-DOGA/DOPC 1:3 (15 and 6 Å, respectively). This is due to the presence of a longer spacer in Ni-NTA-BB molecule (Figure 1). Although the Ni-NTA-BB is diluted with DOPC (ratio 1:3), the effect of this longer linker on the thickness is noticeable.

(36) Parratt, L. G. *Phys. Rev.* **1954**, *95*, 359.

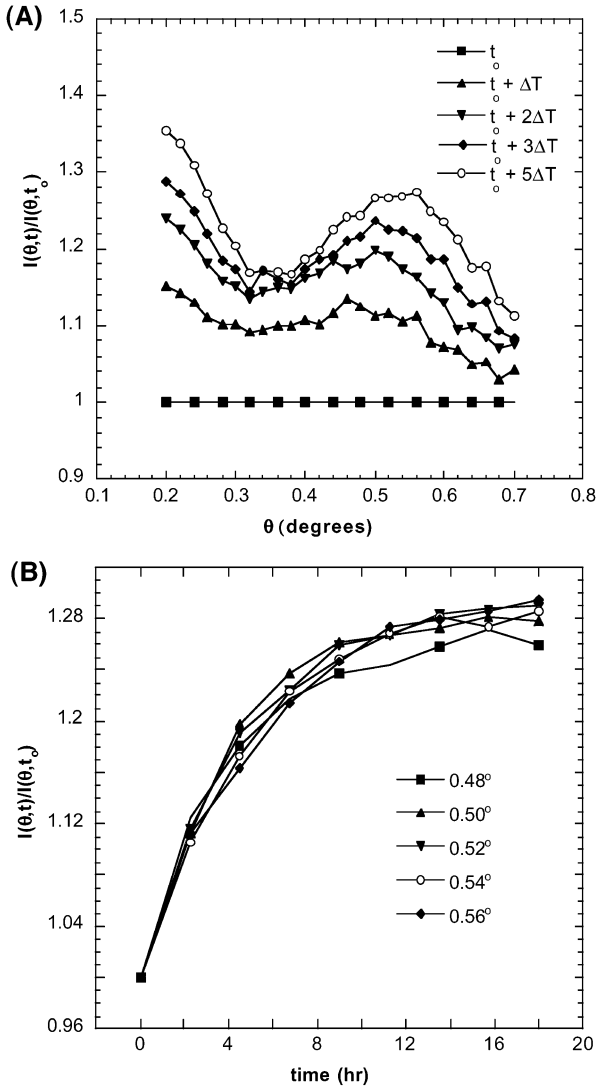

Figure 9. X-ray reflectivity curves during the process of crystallization of HupR on a Ni-NTA-DOGA/DOPC 1:3 lipid monolayer. The protein concentration is 25 μg/mL. Panel A shows successive scans made in the region of the expected position of the Kiessig fringes of a protein layer. Each individual angular scan lasts 135 min, starting at $t = 0$, 135, 270, 405, and 675 min. The wavelength used is $\lambda = 1.54$ Å. Panel B shows the time dependence of the reflected intensities at different angles normalized with the curve measured at $t = 0$ on a lipid layer alone.

Discussion

Protein 2D Crystallization and Monolayer Shear Modulus Value. Invariably, a final high shear modulus value of 58 ± 3 mN/m was indicative of the presence of large crystals of HupR at the air−water interface. Using three different Ni^{2+} lipids at the air−water interface, we found this same value with the presence of large well-ordered crystals on the specimen grids (Table 1, Ni-NTA/DOGA 1:1, 1:3, 1:6; Ni-NTA-BB/DOPC 1:1, 1:3; Ni-NTA-BF/DOPC 1:1). The experiments with BAM described herein have shown that the crystalline patches extend over about 5 μm. This observation is consistent with the data obtained from X-ray grazing incidence measurements done in situ on the 2D crystals of HupR[14] where the size

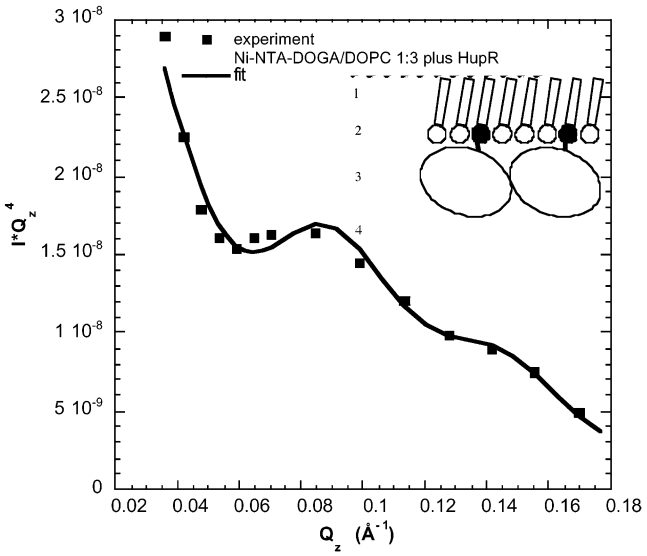

Figure 10. X-ray reflectivity curve measured over a large angular range after completion of HupR protein adsorption on the Ni-NTA-DOGA/DOPC 1:3 lipid monolayer. The solid line corresponds to the best fit with a model (inset) consisting of four layers at the air−water interface: (1) hydrophobic tail of the lipid monolayer; (2) hydrophilic head of the lipid plus the linker; (3) protein; (4) buffer.

Table 2. Values of the Model Parameters Deduced from the X-ray Reflectivity Data of Figures 10 and 11

layer	thickness, d (Å)	electron density (el/Å^3)	roughness (Å)
Ni-DOGA/DOPC 1:3 + HupR			
lipid tail	15	0.35	7
lipid head	6	0.46	7
protein	85	0.35	7
buffer	∞	0.33	7
Ni-NTA-BB/DOPC 1:3 + HupR			
lipid tail	17	0.32	5
lipid head	15	0.39	5
protein	83	0.35	5
buffer	∞	0.33	5
Ni-NTA-BF/DOPC 1:1 + HupR			
lipid tail + head	32	0.34	5
protein	78	0.34	5
buffer	∞	0.33	5

of the crystals at the surface was measured to be bigger than several micrometers. We suggest that the elasticity of the polycrystalline patches results from a mechanical system combining the solid behavior of the crystalline patches in series with the soft grain boundaries between the crystalline patches. On the other hand, we interpret a lower value of the shear elastic constant as the result of disordered adsorption of proteins onto the surface of the lipid monolayer. This difference suggests the change from large crystalline patches of well-ordered proteins (surrounded by thin grain boundaries) toward smaller crystalline patches with more defects or less specificity of interaction between proteins (surrounded by larger and larger noncrystalline areas). A value of 48 mN/m (i.e., Table 1, Ni-NTA-BF/DOPC 1:0) for the shear modulus μ probably indicates in situ a mixture of microscopic crystalline arrangements and randomly interacting proteins; indeed, the observation of electron microscope grids after transfer of these layers shows some very small cristalline patches poorly organized. Small loose crystals are produced but are damaged during the transfer onto specimen grids. A value of 20 mN/m (i.e., Table 1, Ni-NTA-DOGA/DOPC 1:0) for the shear modulus μ corresponds to even weaker interactions between the proteins. For that particular reason, only occasional and very small crystals are observed on the grids in that situation.

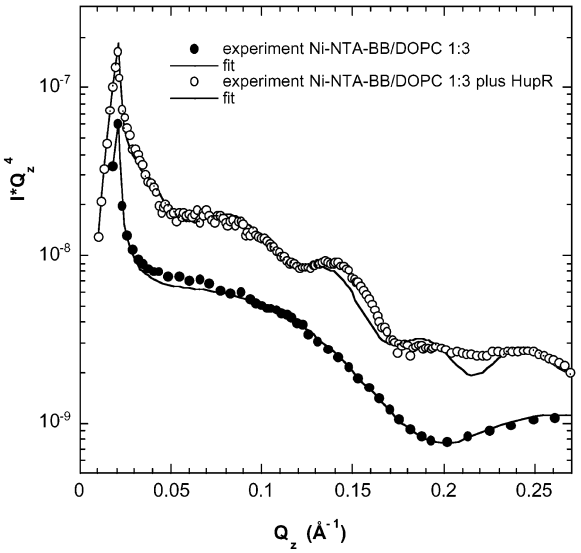

Figure 11. X-ray reflectivity curves measured using the synchrotron radiation on a Ni-NTA-BB/DOPC 1:3 lipid monolayer at the air−water interface (●) before and (○) after incubation on a HupR protein solution (25 μg/mL). The solid lines corresponds to the best fit with a model (see inset Figure 10) consisting of two layers for the lipid tails and heads and one layer for the adsorbed proteins (the parameters of the fit are listed in Table 2).

The shear modulus value μ is a macroscopic measurement that can provide information about the lateral protein−protein interactions. A theoretical limit of the in-plane resolution obtainable with X-ray grazing incidence data can be estimated from the measured value of the shear elastic constant.[14] That value varies from one protein forming 2D crystals at the interface to another. On one hand, very high values of rigidity have been previously reported with 2D crystals of streptavidin adsorbed on biotinylated lipid monolayer (90 mN/m).[14,33] On the other hand, very low shear elastic modulus values have been found when testing the crystallization of annexin V on a dioleoylphosphatidylserine monolayer and cholera toxin B subunit (CTB) on a monolayer incorporating a monosialoganglioside (GM1), 3 and 5 mN/m, respectively.[21]

Lipid Monolayer Fluidity. The fluidity of the lipid monolayer is a key feature in the 2D crystallization experiment.[3] The process of protein crystallization on a lipid layer passes through at least three successive stages: (1) molecular recognition between the protein and the lipid ligand, that is, adsorption of the protein onto the lipid layer, (2) nucleation and growth of crystalline patches, and (3) annealing of the layer. There is a direct correlation between the fluidity of the lipid film and the crystallization process. Once the proteins are adsorbed and concentrated at the lipid layer, the organization of proteins within a 2D crystal results from the in-plane diffusion of the protein−lipid complexes both in rotation and in translation. This diffusion process is controlled by protein−protein interactions and lipid−lipid interactions. The balance between the forces involved determines the fluidity of the protein−lipid layer. However, when the protein−lipid interactions are weak (typically Coulombic interactions), the fluidity of the lipid film is likely to be less crucial because such a weak interaction is easily broken and the protein can then recreate another one with a neighboring lipid. The

resulting dynamic equilibrium allows the protein to move laterally in the plane and eventually compensates for the lack of fluidity of the lipid layer. In the case of the strong interaction existing between a His-tagged protein and a Ni^{2+}-chelating lipid (pH 8, $K_d = 10^{-13}$ [34]) or between any receptor [ligand] couple, the lipid−protein complex once formed is unlikely to break. Then, the only way for the anchored protein to move at the interface is by an in-plane diffusion process of the lipid−protein complex. That definitely commands the use of a fluid lipid monolayer. Consequently, lipids spread in the solid phase at the air−water interface are producing at best a close packing of proteins but in no case 2D crystals.[37] Successful protein 2D crystallizations were always performed on a lipid film in a fluid phase.

In our experiments, although all of the lipids were spread into fluid monolayers at room temperature, in some cases, the shear elastic constant failed to reach the maximum value indicative of crystal formation (Table 1, all of the lipid mixtures that do not give rise to 2D crystals, i.e., Ni-NTA-DOGA/DOPC 1:0, 2:1, 1:12; Ni-NTA-BB/DOPC 1:0, 2:1, 1:12; Ni-NTA-BF/DOPC 1:0, 2:1, 1:3, 1:6, 1:12). In these particular cases, the three-step process mentioned above was not completed, and we can then investigate where this process might have failed. The first stage of the process, that is, adsorption of the protein on the monolayer, did occur. This was monitored by the ellipsometric measurements and observed on the electron microscope grids. The second stage, consisting in the establishment of optimum intermolecular contacts between neighbor proteins, which are essential for growing crystals did not occur. Some protein−protein interactions were certainly present but were not those specific interactions between proteins that are a prerequisite for the growth of a crystal. We propose that the lipid−protein complex is not free enough to diffuse in the plane and cannot establish the appropriate interactions conducive to crystal formation.

A remarkable improvement of the fluidity of the monolayer is achieved by using the branched lipid structure (Ni-NTA-BB) diluted with DOPC (1:1 or 1:3). At a molecular level, the branched and the bent unsaturated chains introduce some perturbations in the packing of the hydrophobic tails. These perturbations increase the fluidity of the monolayer, which enables the right compaction of proteins to take place faster.

When pure Ni-NTA-BF is used, we measured a very high value for the shear elastic constant: 48 compared with 20 and 18 mN/m when pure Ni-NTA-DOGA and pure Ni-NTA-BB are used, respectively. Though the interaction between a branched and a fluorinated chain are repulsive, improving the monolayer fluidity, Ni-NTA-BF alone does not allow the formation of 2D crystal. The only dilution ratio favorable to the growth of large crystals is Ni-NTA-BF/DOPC 1:1. The process of crystallization, however, is slowed when compared with the process when Ni-NTA-DOGA is used. We can explain this phenomena by a possible segregation of the fluorinated chains interacting with each other and preventing a proper mixing with DOPC. Although not successful for the His-HupR crystallization, the fluidity of the monolayer has been increased, and this lipid could be a good candidate when trying to crystallize other His-tagged proteins.

Conclusion

The meticulous and systematic study of the 2D crystallization process presented herein is especially important to improve our understanding of the different steps involved in the self-organization of a His-tagged protein on a Ni^{2+}-chelating lipid monolayer. In this study, we have shown that both the crystallization rate and the quality of the resulting crystals depend to a considerable extent on the fluidity properties of the lipid matrix. New original branched and semifluorinated lipids have been evaluated. The branched Ni^{2+}-functionalized lipid **2** appears to be an especially good candidate for general use in the 2D crystallization of His-tagged proteins. This lipid improves the kinetics of adsorption of the His-tagged protein onto the lipid monolayer and accelerates the rate of crystal formation. Making the crystallization faster is of special importance for fragile and easily degradable proteins at room temperature. Finally, ellipsometric angle and shear rigidity measurements, X-ray reflectivity, and Brewster angle microscopy prove to be valuable and complementary tools when investigating protein 2D crystallization.

Acknowledgment. S.C. was supported by a grant from MENESR (France). We are grateful to Jens Dietrich for his critical reading of the manuscript.

LA026261Z

(37) Mosser, G.; Brisson, A. *J. Struct. Biol.* **1991**, *106*, 191.